INVESTIGATION OF A FAMILY OF SIMPLY PERIODIC ORBITS AROUND THE MOON OF MARS

Abdullah A. Ansari
Department of Mathematics, College of Science, Majmaah University, Al-Zulfi, KSA.
a.ansari@mu.edu.sa

ABSTRACT: *This paper presents the investigation of a family of simply periodic orbits around the moon of the Mars, for which we have considered the circular restricted three body problem where one of the primaries is taken as Mars and other one as moon of the Mars (Phobos) and third infinitesimal body as satellite and also both primaries are taken as oblate. We have considered the effect of Poynting-Robertson drag from one of the primaries (Mars) to the satellite. We have evaluated the equations of motion of the satellite under the effect of P-R drag and oblateness. We also have plotted the equilibrium points, periodic orbits, zero-velocity curves, Poincare surfaces of section and finally the basins of attraction for the different values of oblatenes and mass reduction factor. It is observed that we got atmost five equilibrium points which are moving on the variation of the perturbing factors, the orbits are periodic, the zero-velocity curves are different for the different perturbations, the Poincare-surfaces of section occurred variations on the variation of the perturbing factors and finally in the basins of attraction, we got different color code for the equilibrium points on the variation of the perturbing factors.*

1. INTRODUCTION

Last many decades the restricted problem was the attractive problem for scientists especially in physics, astronomy and mathematics. During the study of these problems, they have considered many perturbations like oblateness, solar radiation pressure, drags, variation of masses, yarkovsky effect, albedo, Coriolis and centrifugal forces etc. This problem is significant in various fields, particularly to the field of astrodynamics, astronomy and astrophysics. Many researchers studied on restricted three-body problem like Radzievskii [1], Bhatnagar [2], Sharma [3], Singh [4, 5], Simmons [6], Kumar [7], Hadjidemetriou [8], Ragos [9], Hallan [10, 12], Kalvouridis [11], Raheem [13], Baltagiannis [14], Zhang [15], Abouelmagd [16], Jain [17], Mishra [18], Ansari [19] etc. have studied in the restricted problem with perturbations. The restricted problem has helped in determining the families of simple periodic orbits, nature of the stability around the hyperbolic Lyapunov periodic orbits, stability of the libration points etc.

Taking on consideration, we have investigated the family of simply periodic orbits around moon of the Mars. Here we have considered the restricted three body problem as a model where one of the primaries is considered as oblate Mars, other one as oblate moon of the Mars (Phobos) and infinitesimal body as satellite. All the numerical values have been taken from Zamaro [20].

This paper contains four sections considering introduction as first section. In the second section, we have determined the equations of motion of the satellite. In the third section, we have done all the computational work. And finally in the fourth section, we have concluded the problem.

2. EQUATIONS OF MOTION

Let there be three masses m_1, m_2 and m ($m_1 \geq m_2$). Here m_1, m_2 and m are considered as the masses of oblate Mars, oblate moon of Mars (Phobos) and satellite respectively with oblateness factors σ_1 (Mars) and σ_2 (Phobos), and also the effect of Poynting-Robertson drag (F_{PRD}) is taken from Mars to satellite. The line joining the masses m_1 and m_2 has been chosen as ξ-axis. They revolve in circular orbits with the angular velocity $'\omega'$ without rotation about their common Centre of mass O which has been taken as origin and the line perpendicular to ξ-axis through origin in the plane of motion of the primaries is taken as η-axis. The line through origin and perpendicular to the plane of motion of the primaries is taken as ζ-axis. Let us consider a synodic system of coordinates, initially coincident with the inertial system, rotating with angular velocity ω about ζ-axis.

We, now assume that $\dfrac{m_2}{m_1 + m_2} = \mu$ and choose units of mass, length and time such that $m_1 + m_2 = 1$, l (distance between the primaries) $= 1$ and $G = 1$ respectively. Let masses $m_2 = \mu$ and hence $m_1 = 1 - \mu$. The co-ordinates of the locations of the masses are (μ, 0, 0) (Mars), (-(1- μ), 0, 0) (Phobos) and (ξ, η, ζ) (satellite). Therefore, the equations of motion of satellite in the non-dimensional variables are
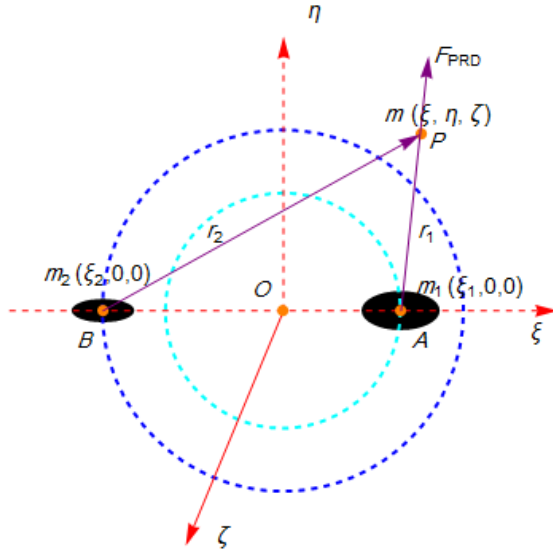
Figure-1: Geometry of the problem.

$$\ddot{\xi} - 2n\,\dot{\eta} = U_{\xi} + F_{PRD\xi} = \Omega_{\xi},,$$

$$\ddot{\eta} + 2n\dot{\xi} = U_{\eta} + F_{PRD\eta} = \Omega_{\eta},,$$

$$\ddot{\zeta} = U_{\zeta} + F_{PRD\zeta} = \Omega_{\zeta}. \tag{1}$$

where

$$\Omega = \frac{n^2}{2}\left(\xi^2 + \eta^2\right)$$

$$+ \left(\frac{(1-\mu)q_1}{r_1} + \frac{\mu}{r_2} + \frac{(1-\mu)\sigma_1}{2r_1^3} + \frac{\mu\sigma_2}{2r_2^3}\right)$$

$$+ W_1\left(\frac{(\xi - \mu)\dot{\xi} + \eta\dot{\eta} + \zeta\dot{\zeta}}{2r_1^3} - n\,\arctan(\frac{\eta}{\xi - \mu})\right),$$

$$W_1 = \frac{(1-\mu)(1-q_1)}{c_d},$$

$$r_1^2 = \left(\xi - \mu\right)^2 + \eta^2 + \zeta^2,$$

$$r_2^2 = \left(\xi + 1 - \mu\right)^2 + \eta^2 + \zeta^2,$$

q_1 is mass reduction factor and $n^2 = (1 + \frac{3}{2}(\sigma_1 + \sigma_2))$.

3. COMPUTATIONAL WORKS
In this section, we have plotted equilibrium points, periodic orbits, zero-velocity curves, Poincare surfaces of section and the basins of attraction for the different values of oblateness and the mass reduction factor through Mathematica software ($m_1 = 6.42*10^{23}$, $\sigma_1 = 0.00196$ (Mars), $m_2 = 1.07*10^{16}$, $\sigma_2 = 0.105$ (Phobos)) (Zamaro [20]).

3.1 Equilibrium Points
We can find the equilibrium points from equation (1) by

putting $\ddot{\xi} = \dot{\xi} = 0$, $\ddot{\eta} = \dot{\eta} = 0$, $\ddot{\zeta} = \dot{\zeta} = 0$,

i.e. $\quad \Omega_{\xi} = 0, \Omega_{\eta} = 0, \Omega_{\zeta} = 0.$

3.1.1 Equilibrium Points during in-plane motion $(\xi, \eta, \zeta \neq 0)$.
In this plane, we have drawn the equilibrium points in two cases. Firstly the variation of oblatenes (Figure 2(a)) and secondly, the variation of mass reduction factor (Figure 2(b), (c)). From the figure 2(a), we observed that as we increase the values of oblateness, the points move toward the origin and from the figure 2(b, c), as we increase the values of mass reduction factor, the points move away from the origin. In all the figures, orange points denote the locations of the primaries.
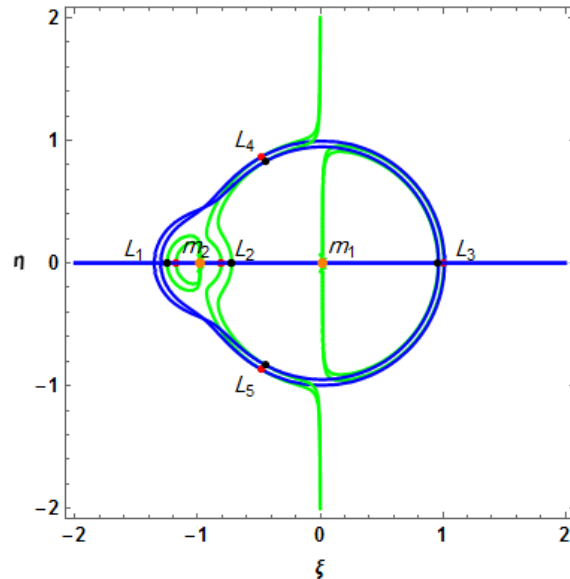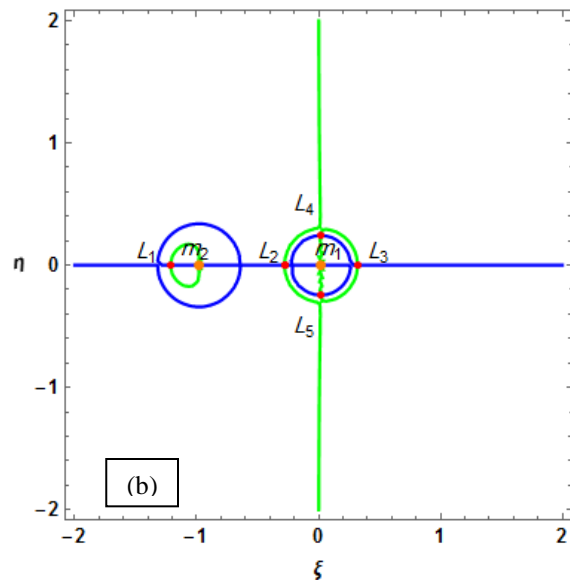

Figure 2(a): Equilibrium points with the variations of oblateness ($\sigma_1 = 0$, $\sigma_2 = 0$ (red), $\sigma_1 = 0.00196$, $\sigma_2 = 0.105$ (black)).
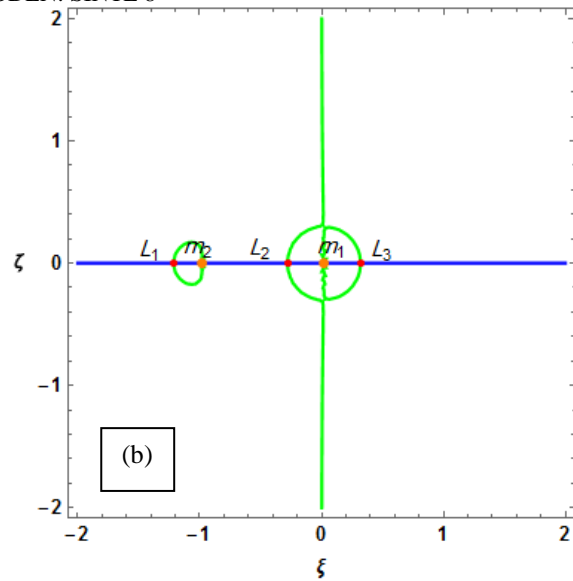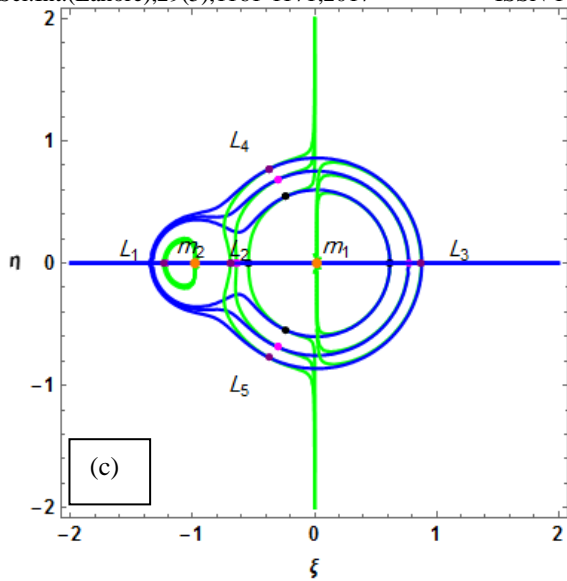
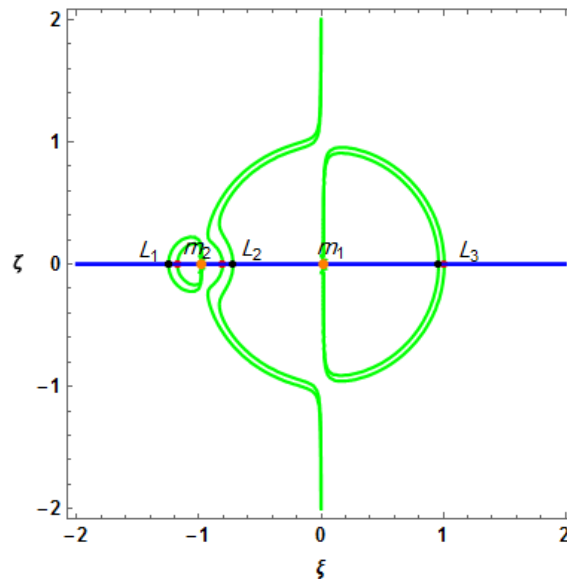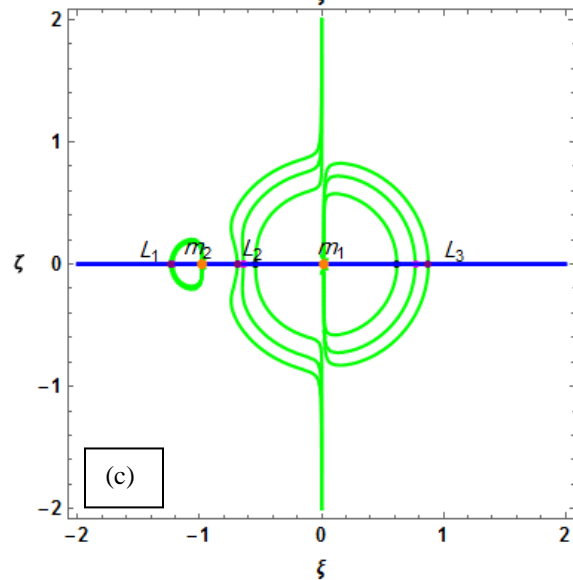**Figure 2: (b) equilibrium points at q_1=0 (red), (c) equilibrium points at q_1=0.25 (black), q_1=0.50 (magenta), q_1=0.75 (purple).**

3.1.2 Equilibrium Points during out of plane motion $(\xi, \eta \neq 0, \zeta), (\xi \neq 0, \eta, \zeta)$.

In these planes, we have got the same pattern, ie. When we increase the values of oblateness, the equilibrium points move towards the origin (Figure 3(a), 4(a)) and after increase the values of mass reduction factor, the equilibrium points move away from the origin (Figure 3(b, c), 4(b)).

Figure 3(a): Equilibrium points with the variations of oblateness ($\sigma_1 = 0$, $\sigma_2 = 0$ (red), $\sigma_1 = 0.00196$, $\sigma_2 = 0.105$ (black)).
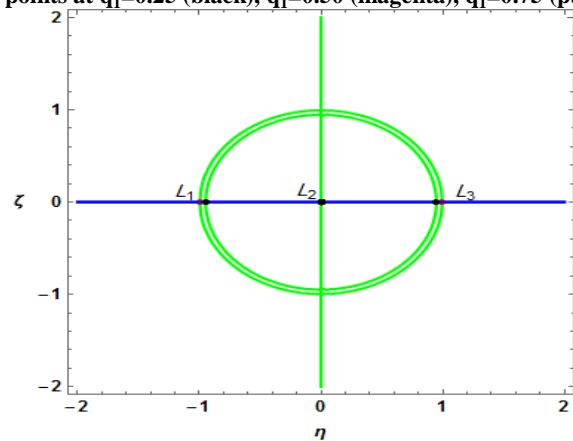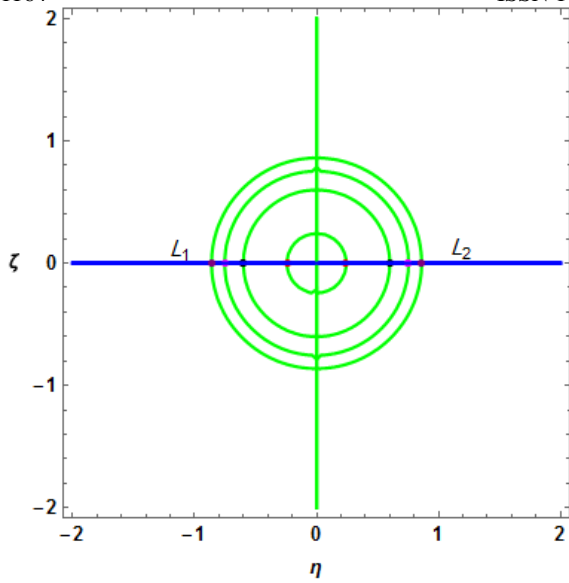

Figure 3: (b) equilibrium points at q_1=0 (red), (c) equilibrium points at q_1=0.25 (black), q_1=0.50 (magenta), q_1=0.75 (purple).

Figure 4(a): Equilibrium points with the variations of oblateness ($\sigma_1 = 0$, $\sigma_2 = 0$ (red), $\sigma_1 = 0.00196$, $\sigma_2 = 0.105$ (black)).

Figure 4: (b) equilibrium points at q_1=0 (red), q_1=0.25 (black), q1=0.50 (magenta), q1= 0.75 (purple).

Figure 5(b): Exotic quasi-periodic orbits with oblateness (σ_1 = 0.00196, σ_2 = 0.105 (black)).

3.2. Periodic Orbit

We have drawn the periodic orbits for the variations of oblateness and mass reduction factor and found the periodic orbits in all the cases. In figures 5(a) and 5(b), we got exotic quasi-periodic orbits and also observed that when we increase the values of oblateness factor, the time period of the periodic orbits reduce. In figure 5(c), we got simply periodic orbits except the case when q_1 = 0.75 (in this case, we got doubly periodic orbits (purple)) and observed that when we increase the values of the mass reduction factor, the periodic orbits shrink.
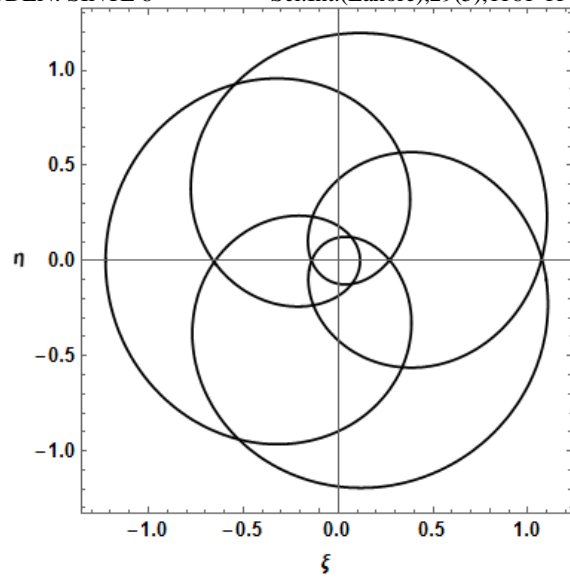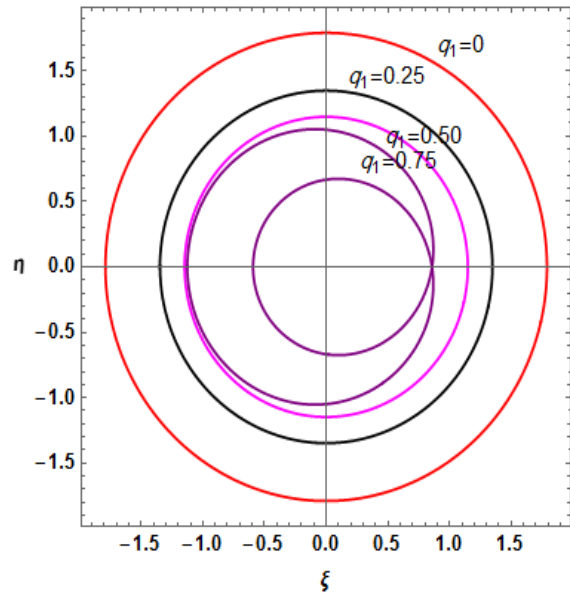

Figure 5(c): Periodic orbits with the variations of mass reduction factor (q_1=0 (red)(simply periodic orbits), q_1=0.25 (black) (simply periodic orbits), q_1=0.50 (magenta) (simply periodic orbits), q_1=0.75 (purple) (doubly periodic orbits)).
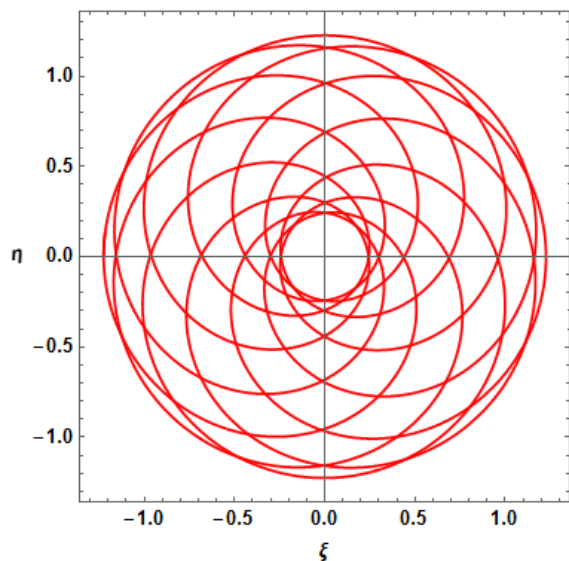
3.3. Zero-velocity curves

We have drawn the zero velocity curves for the variations of oblateness and mass reduction factor and found the different curves for the different values of perturbations (Figures 6(a, b, c, d, e, f)).
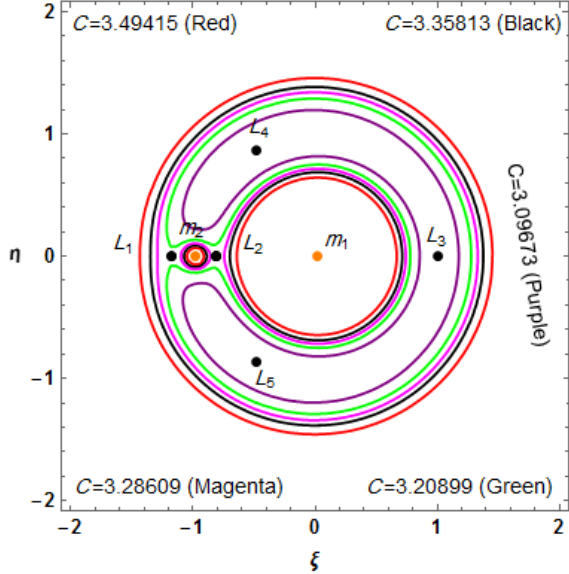

Figure 5(a): Exotic quasi-periodic orbits without oblateness (σ_1 = 0, σ_2 = 0 (red)).

Figure 6(a): Zero velocity curves without oblateness
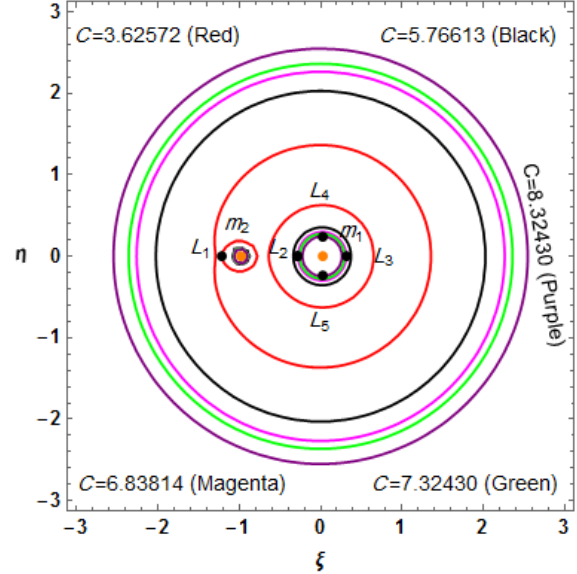$(\sigma_1 = 0, \sigma_2 = 0, q_1 = 1)$.

Figure 6(c): Zero velocity curves without mass reduction factor
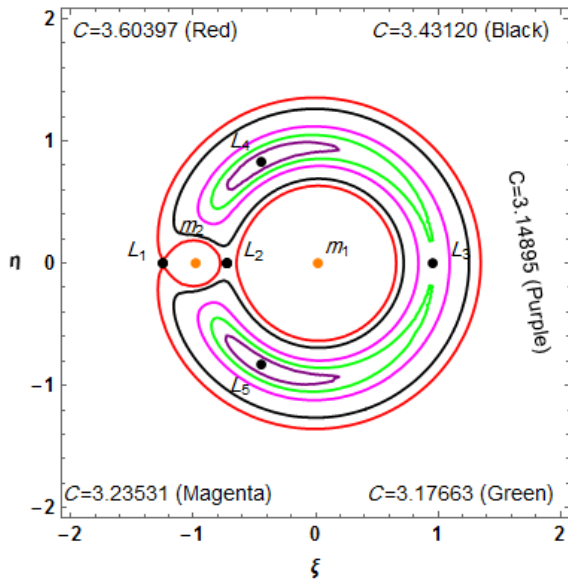$(q_1 = 0, \sigma_1 = 0.00196, \sigma_2 = 0.105)$.

Figure 6(b): Zero velocity curves with oblateness
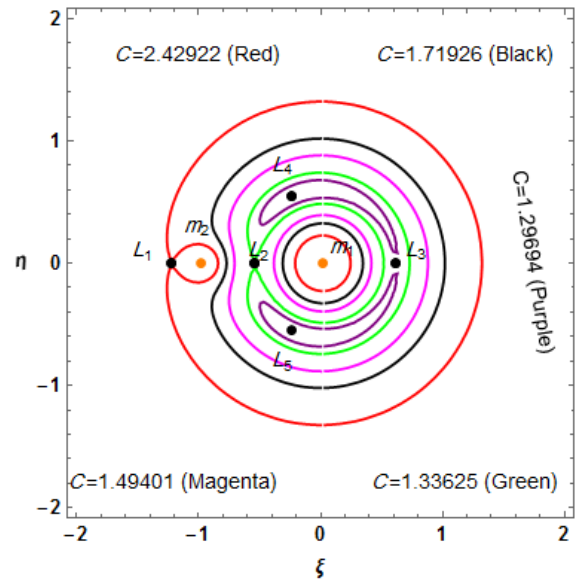$(\sigma_1 = 0.00196, \sigma_2 = 0.105, q_1 = 1)$.

Figure 6(d): Zero velocity curves with mass reduction factor
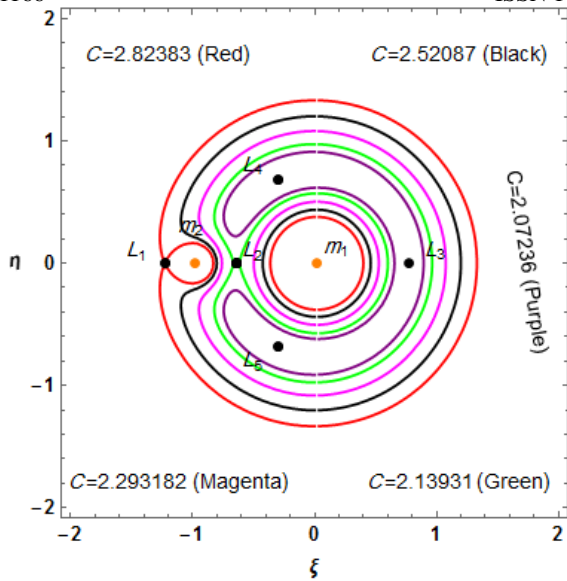$(q_1 = 0.25, \sigma_1 = 0.00196, \sigma_2 = 0.105)$.

Figure 6(e): Zero velocity curves with mass reduction factor
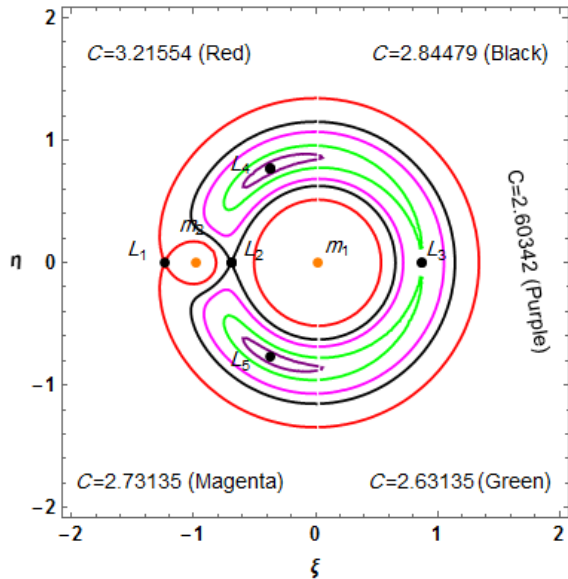$(q_1 = 0.50, \sigma_1 = 0.00196, \sigma_2 = 0.105)$.

Figure 6(f): Zero velocity curves with mass reduction factor
$(q_1 = 0.75, \sigma_1 = 0.00196, \sigma_2 = 0.105)$.

3.4. Poincare surfaces of section

We have drawn the Poincare surfaces of section for the variations of oblateness and mass reduction factor and found the different curves for the values of perturbations. (Figures 7(a, b, c)). From figure 7(a), we observed that as we increase the values of oblateness, the surfaces of section expand. From figure 7(b), we observed that, for the small mass reduction factor, the surfaces of section have very large plane and appear as discrete type. From figure 7(c), we observed that as we increase the values of mass reduction factor the surfaces of section expand.
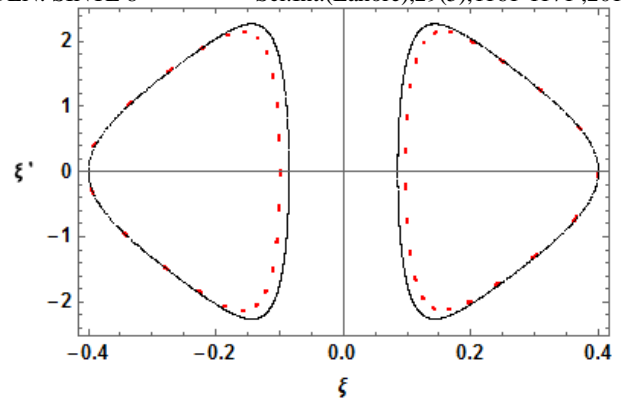

Figure 7(a): Poincare surfaces of section with the variations of oblateness $(\sigma_1 = 0, \sigma_2 = 0, q_1 = 1 \text{ (Red)}), (\sigma_1 = 0.00196, \sigma_2 = 0.105, q_1 = 1 \text{ (Black)})$.

Figure 7(b): Poincare surfaces of section with the variations of mass reduction factor $(\sigma_1 = 0.00196, \sigma_2 = 0.105, q_1 = 0 \text{ (Red)})$, $(\sigma_1 = 0.00196, \sigma_2 = 0.105, q_1 = 0.25 \text{ (Black)})$.

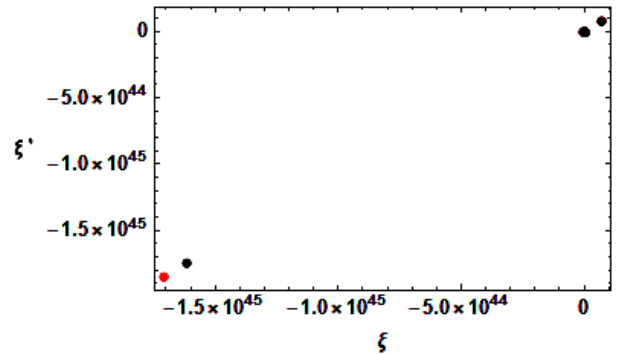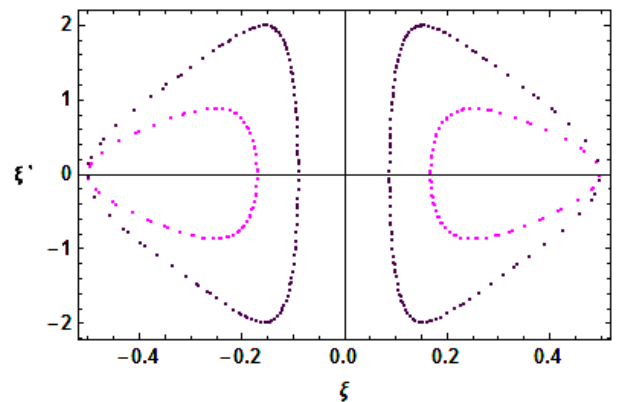**Figure 7(c): Poincare surfaces of section with the variations of mass reduction factor** $(\sigma_1 = 0.00196, \sigma_2 = 0.105, q_1 = 0.50 \text{ (Magenta)}), (\sigma_1 = 0.00196, \sigma_2 = 0.105, q_1 = 0.75 \text{ (Purple)})$.

3.5. Basins of Attraction

In this section, we have drawn the basins of attraction for the variations of oblateness and mass reduction factor by using the simple and accurate Newton-Raphson iterative method for solving systems of equation. This method is also applicable for systems of multivariate functions. The iterative algorithm of our problem is given by the system

$$\xi_n = \xi_{n-1} - \left(\frac{\Omega_\xi \Omega_{\eta\eta} - \Omega_\eta \Omega_{\xi\eta}}{\Omega_{\xi\xi}\Omega_{\eta\eta} - \Omega_{\xi\eta}\Omega_{\eta\xi}} \right)_{(\xi_{n-1},\eta_{n-1})} ,$$

$$\eta_n = \eta_{n-1} - \left(\frac{\Omega_\eta \Omega_{\xi\xi} - \Omega_\xi \Omega_{\eta\xi}}{\Omega_{\xi\xi}\Omega_{\eta\eta} - \Omega_{\xi\eta}\Omega_{\eta\xi}} \right)_{(\xi_{n-1},\eta_{n-1})} . \quad (5)$$

Where ξ_{n-1}, η_{n-1} are the values of the ξ and η coordinates of the (n-1)$_{th}$ step of the Newton-Raphson iterative process. The initial point (ξ,η) is a member of the basin of attraction of the attractor if this point converges rapidly to one of the equilibrium points. This process stops when the successive approximation converges to an attractor, with some predefined accuracy. For the classification of the equilibrium points on the (ξ,η) plane, we will use color code. In this way a complete view of the basin structures created by the attractors. (Figures (8, 9, 10, 11, 12, 13))

We can observe in detail from the zoomed part of all the figures in Fig. 8(b), Fig. 9(b), Fig. 10(b), Fig. 11(b), Fig. 12(b), Fig. 13(b). The red points and orange points denote the locations of the lagrangian points and the primaries respectively.
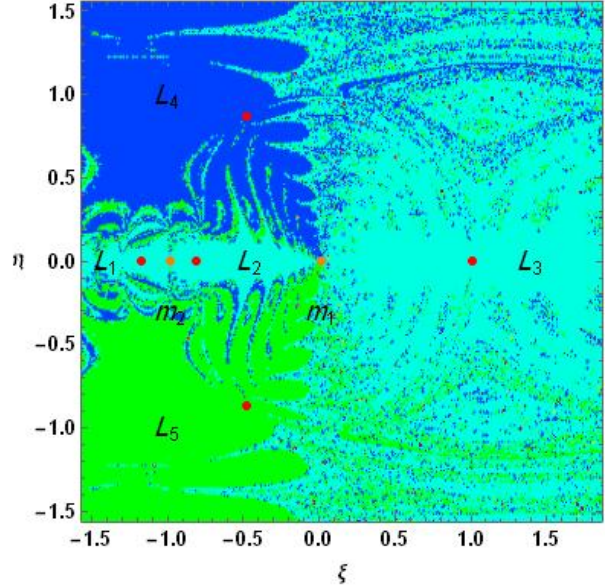

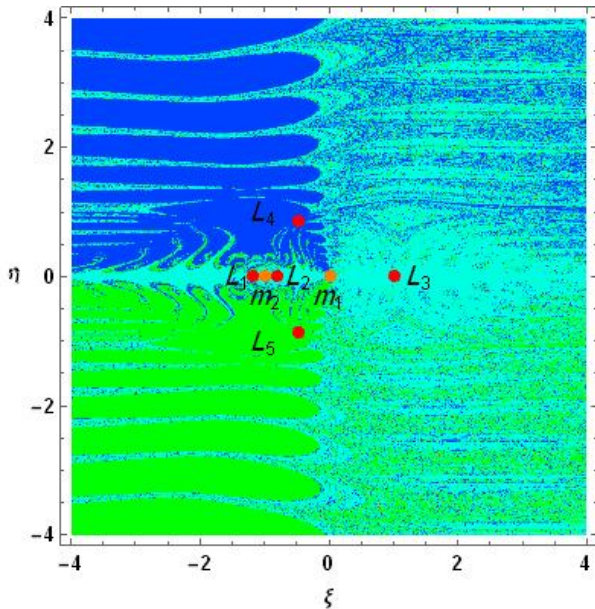**Figure 8(b): Zoomed part of figure 8(a) near the primaries.**

Figure 9(a): Basins of attraction with oblateness ($\sigma_1 = 0.00196$, $\sigma_2 = 0.105$, $q_1 = 1$).
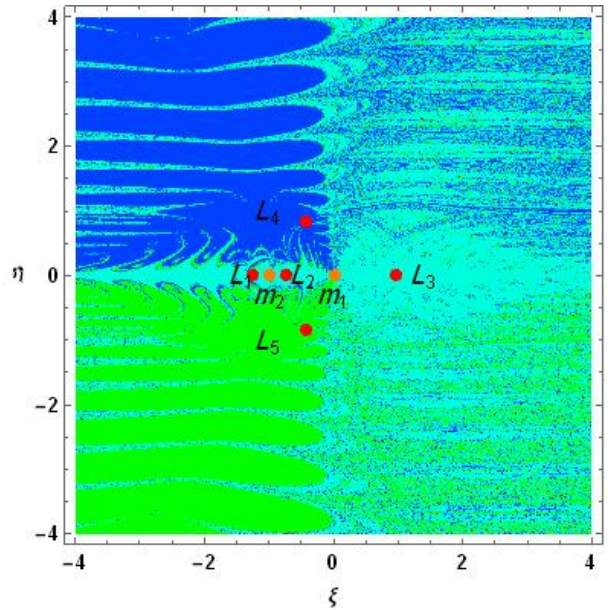

Figure 8(a): Basins of attraction without oblateness ($\sigma_1 = 0$, $\sigma_2 = 0$, $q_1 = 1$).

Figure 9(b): Zoomed part of figure 9(a) near the primaries.

Figure 10(b): Zoomed part of figure 10(a) near the primaries.

Figure 10(a): Basins of attraction without mass reduction factor ($\sigma_1 = 0.00196$, $\sigma_2 = 0.105$, $q_1 = 0$).

Figure 11(a): Basins of attraction with the mass reduction factor ($\sigma_1 = 0.00196$, $\sigma_2 = 0.105$, $q_1 = 0.25$).
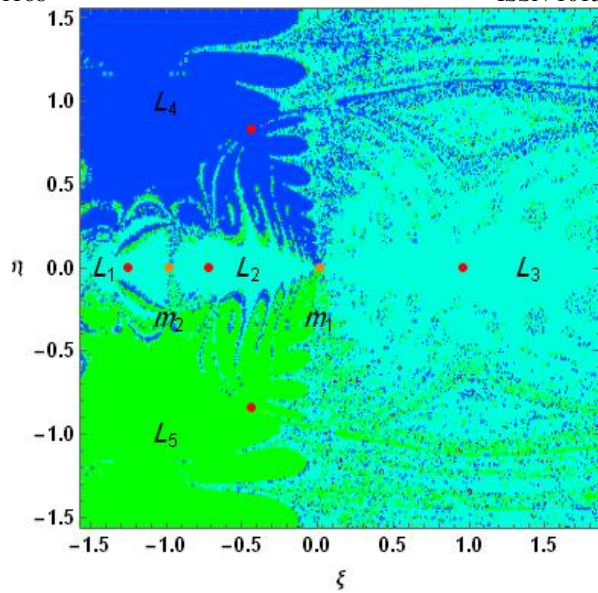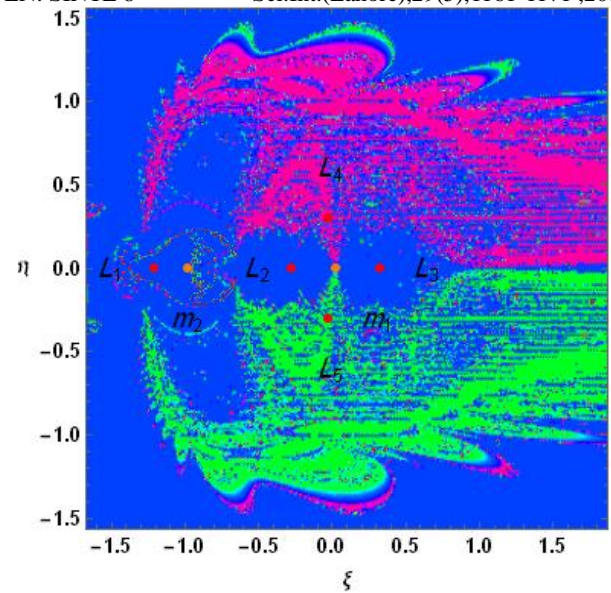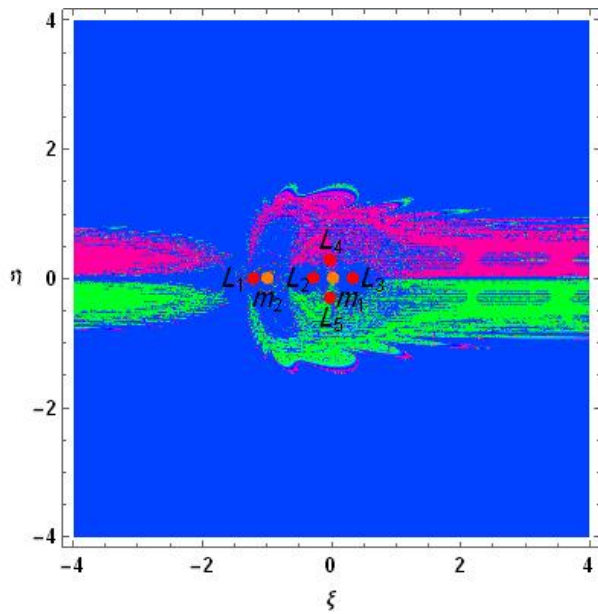
Figure 11(b): Zoomed part of figure 11(a) near the primaries.

Figure 12(b): Zoomed part of figure 12(a) near the primaries.

Figure 12(a): Basins of attraction with the mass reduction factor ($\sigma_1 = 0.00196$, $\sigma_2 = 0.105$, $q_1 = 0.50$).
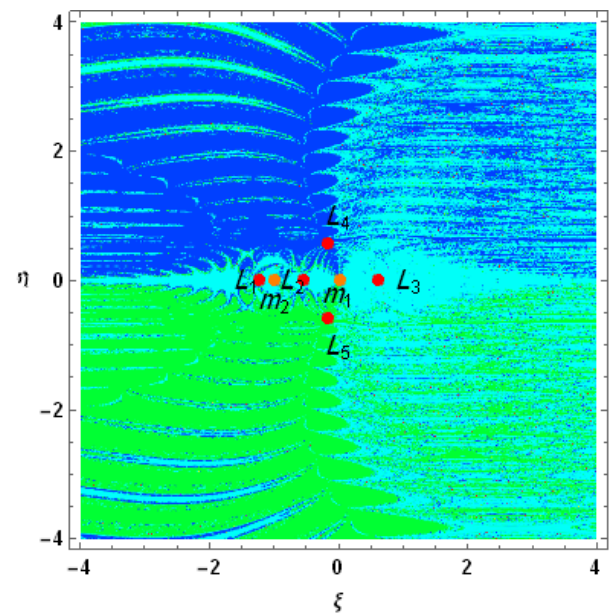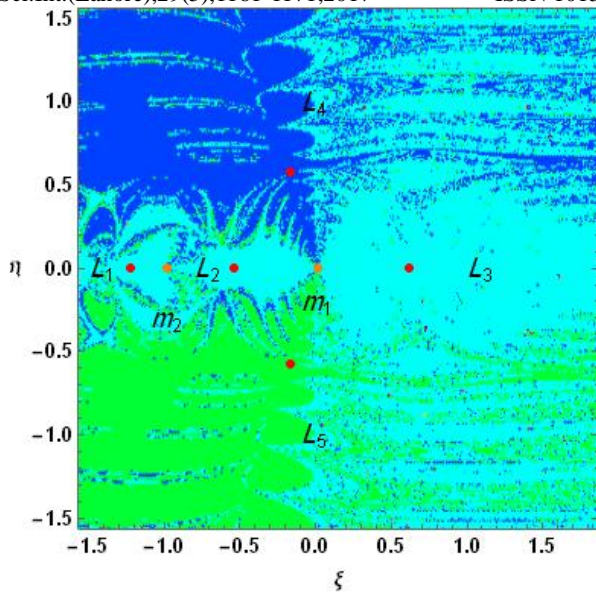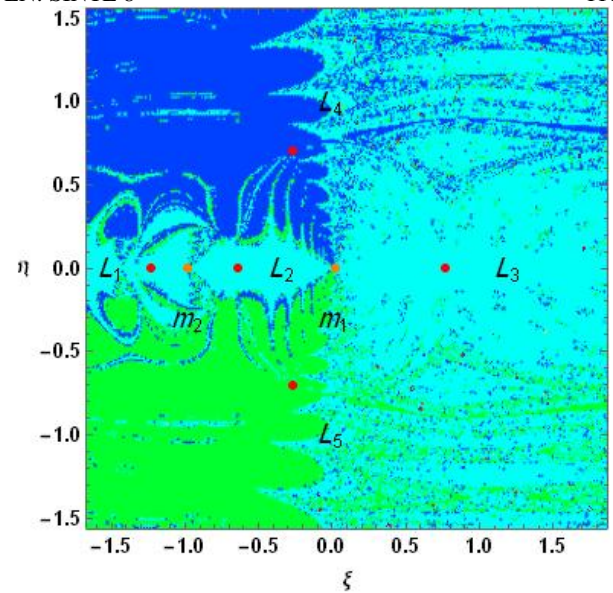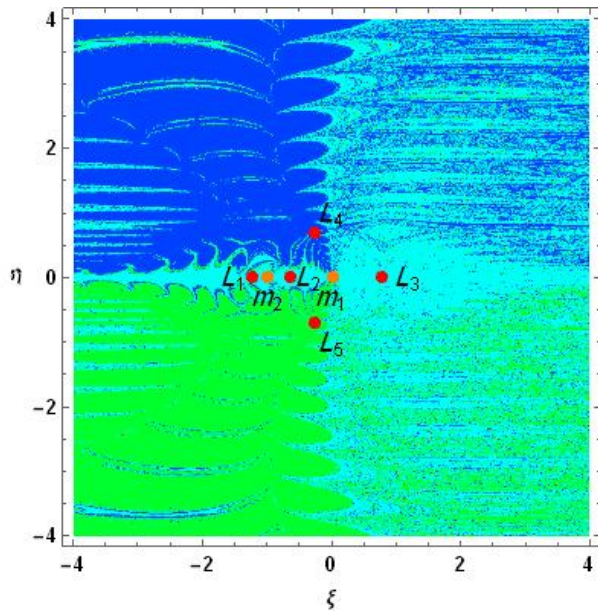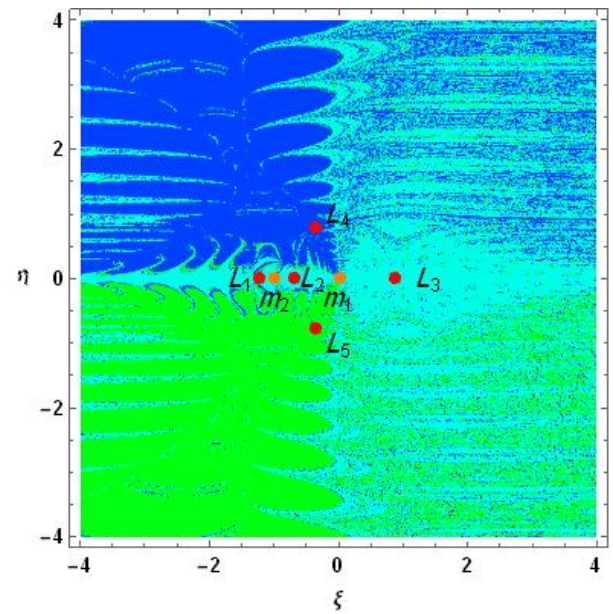

Figure 13(a): Basins of attraction with the mass reduction factor ($\sigma_1 = 0.00196$, $\sigma_2 = 0.105$, $q_1 = 0.75$).
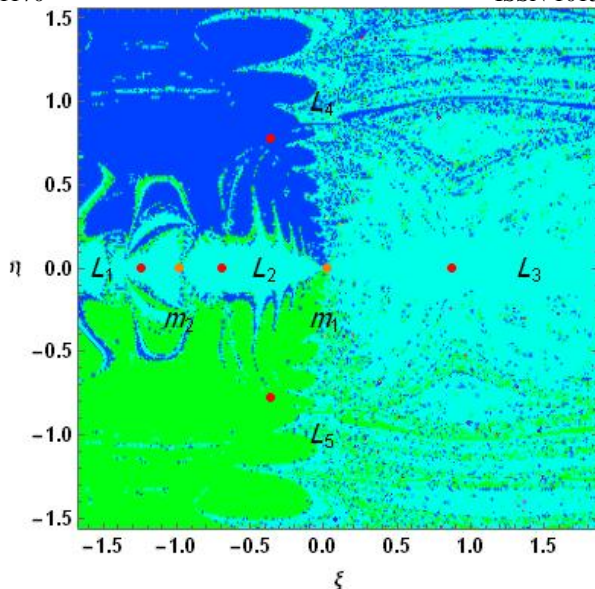
Figure 13(b): Zoomed part of figure 13(a) near the primaries.

4 CONCLUSION AND DISSCUSSION

We have investigated the family of simply periodic orbits around the moon of Mars (Phobos). For this we have considered the circular restricted three body problem in which one of the primaries is taken as oblate Mars, other one as oblate moon of the Mars (Phobos) and third infinitesimal body is taken as satellite. We have taken the effect of P-R drag from Mars to satellite. By using the equations of motion, we have drawn the equilibrium points in and out-of-plane and observe that these points are moving with the variations of oblateness and mass reduction factor. On the other hand, we found the exotic quasi periodic orbits, doubly periodic orbits and simply periodic orbits. In the zero velocity curves the satellite will move only in the particular region of the whole region. In the Poincare surfaces of section, we got the variations with the variations of perturbing factor. And finally, we have plotted the basins of attraction for this problem by using Newton Raphson iterative method through Mathematica software and found different color code for different equilibrium points. It can be clearly seen in zoomed part of all the figures.

In this way, reader can get very much interesting infor mation about the motion of the satellite around the moon of Mars.

REFERENCES

1. Radzievskii, V.V. (1953) The Space Photogravitational Restricted Three-Body Problem. Astronomical Journal, 30, 225.
2. Bhatnagar, K.B., Hallan, P.P. (1978) Effect of perturbations in Coriolis and centrifugal forces on the stability of libration points in the restricted problem. Celest. Mech. 18, 105-112.
3. Sharma, R. K., (1982) On linear stability of triangular libration points of the photogravitational restricted three body problem when the more massive primary is an oblate spheroid, Sun and Planetary System, W. Fricke and G. Teleki (eds), 435-436.
4. Singh, J., Ishwar, B. (1984) Effect of perturbations on the location of equilibrium points in the restricted problem of three bodies with variable mass. Celest. Mech. 32(4), 297-30.
5. Singh, J., Ishwar, B. (1985) Effect of perturbations on the stability of triangular points in the restricted problem of three bodies with variable mass. Celest. Mech. 35, 201-207.
6. Simmons, JFL., Mcdonald, AJC. and Brown, JC (1985) The restricted three body problem with radiation pressure. Celest. Mech. 35, 145.
7. Kumar, V. and Chaudhary, R.K. (1986) Existence of libration points in the generalized photogravitational restricted problem of three bodies. Celest. Mech. 39, 159-171.
8. Hadjidemetriou, J. D., (1988) Periodic orbits of planetary type and their stability, Celest. Mech. (KAP), 43, 371-390.
9. Ragos, O., Zagouras, C., (1988) Periodic solutions about the out of plane equilibrium points in the photogravitational restricted three body problem, Celest. Mech. 44, 135-154.
10. Hallan, P. P. and Rana, N. (2001) Effect of perturbations in coriolis and centrifugal forces on the location and stability of the equilibrium point in the Robe's circular restricted three body problem. Planetary and Space Science, vol. 49, no. 9, pp. 957–960.
11. Kalvouridis, T.J., Arribas, M., Elipe, A. (2007) Parametric evolution of periodic orbits in the restricted four-body problem with radiation pressure. Planet. Space Sci. 55, 475-493, DOI 10.1016/j.pss.2006.07.005.
12. Hallan, P. P. and Mangang, K. B. (2008) Effect of perturbations in coriolis and centrifugal forces on the Nonlinear Stability of Equilibrium point in Robe`s Restricted Circular Three body Problem. Advances in Astronomy, 21.
13. Raheem, A., Singh, J. (2008) Combined effects of perturbations, radiations and oblateness on the periodic orbits in the restricted three body problem. Astrophys. Space Sci. 317, 9-13.
14. Baltagiannis, A.N., Papadakis, K.E. (2011) Equilibrium points and their stability in the restricted four-body problem. International Journal of Bifurcation and Chaos 21, 2179, DOI10.1142/S0218127411029707.
15. Zhang, M. J., Zhao, C. Y., Xiong, Y. Q. (2012) On the triangular libration points in photogravitational restricted three-body problem with variable mass.

Astrophysics Space Sci. 337, 107-113, DOI 10.1007/s10509-011-0821-8.

16. Abouelmagd, E.I., Mostafa, A. (2015) Out of plane equilibrium points locations and the forbidden movement regions in the restricted three-body problem with variable mass. Astrophysics and Space Sci. 357, 058, DOI 10.1007/s10509-015-2294-7.

17. Jain, P. Aggarwal, R., Mittal, A., Abdullah, (2016) Periodic orbits in the photogravitational restricted problem when the primaries are triaxial rigid body, International Journal of Astronomy and Astrophysics, 6(1), 111-121.

18. Mishra, V. K., Sharma, J. P., Ishwar, B., (2016) Stability of triangular equilibrium points in the photogravitational elliptic restricted three body problem with Poynting-Robertson drag, International Journal of Advanced Astronomy, 4(1), 33-38.

19. Ansari, A. A., Kellil, R. (2017) Periodic motion of Martian moon's satellite, Nonlinear Sci. Lett. A, 8(2), 171-177.

20. Zamaro, M., Biggs, J. D. (2015), Natural motion around the Martian moon Phobos: The dynamical substitutes of the libration point orbits in an elliptic three-body problem with gravity harmonics, Celest. Mech. Dyn. Astr. 122: 236-302, DOI 10.1007/s 10569-015-9619-2.